Enhanced Hall effect in Co/Pd multilayered nanodomes with perpendicular anisotropy

Sebastian Michea, Simón Oyarzún, Sorach Vidal, and Juliano C. Denardin

Enhanced Hall effect in Co/Pd multilayered nanodomes with perpendicular anisotropy

Sebastian Michea,[1,2] Simón Oyarzún,[1,2] Sorach Vidal,[1] and Juliano C. Denardin[1,2,a]

[1]*Departamento de Física, Universidad de Santiago de Chile (USACH), Avda. Ecuador 3493, 917-0124 Santiago, Chile*
[2]*Center for the Development of Nanoscience and Nanotechnology (CEDENNA), 917-0124 Santiago, Chile*

In this work, multilayers of Co/Pd with out of plane anisotropy have been deposited on the bottom of porous alumina membranes, forming nanodomes films with 100 and 200 nm diameter. The magnetization reversal of the multilayers is investigated by magnetization curves, extraordinary Hall effect and magnetic force microscopy (MFM) experiments. The results show that as the pore diameter increase, a larger hall resistivity is obtained, compared with the continuous film. © *2017 Author(s). All article content, except where otherwise noted, is licensed under a Creative Commons Attribution (CC BY) license (http://creativecommons.org/licenses/by/4.0/).* [http://dx.doi.org/10.1063/1.4975489]

I. INTRODUCTION

Magnetic thin films with perpendicular magnetic anisotropy (PMA) are very important in the recording[1–3] and as magnetic sensors industries.[4,5] The research and potential applications of nano-patterned PMA films is still more exciting, since the patterns can have length scales similar to the domain-wall widths and can be tailored to limit the domain-wall propagation,[6–8] and to observe new magnetic phenomena as magnetic skyrmions.[9] Methods for fabrication of nanopaterned PMA films include lithography or self-assembling block copolymers.[3,5,10] E-beam lithography techniques are expensive and slow, and self-assembling of nanospheres presents problems with both dislocations and adhesion to the substrates. Among the ways to produce nanostructured films, anodized alumina templates (AAO) have emerged as a low cost, simple and effective method to obtain large areas of nanopatterns.[6,11] When a material is deposited on top of AAO membranes with pores of different diameter a continuous film with an arrangement of holes is obtained. However, if we use the bottom side of AAO membranes (barrier layer) we can obtain nanohills or nanodomes films, where the last one shows different magnetic reversion mechanisms and can be interesting in basic and applied research in magnetism. PMA Co/Pt multilayers deposited on alumina barrier layers, forming nanobumps, have been studied before,[12,13] but only bump periods inferior to 100 nm have been analyzed. Larger period with curved surfaces have been studied by deposition of Co/Pd films on self-assembled SiO_2 nanospheres,[5] but with the associated problems mentioned above that are a limiting factor for magnetotransport studies.

In this work we use the bottom side of nanostructured AAO membranes fabricated with pore diameters of 100 nm and 250 nm as substrates for deposition of Co/Pd multilayers. The magnetic domain configuration was observed by magnetic force microscopy (MFM), and magnetic and magnetotransport properties of the nanostructured films were studied by magnetometry and Hall effect measurements.

---

[a]Electronic mail: juliano.denardin@usach.cl.

II. EXPERIMENTAL METHOD

The fabrication process of magnetic nanodomes is composed of a three-stage method where the film is deposited onto the barrier layer of nanoporous alumina membranes (NAMs).[12] The first step consists of the fabrication of NAMs by double anodization technique[14,15] and subsequent removal of the remaining Al by chemical etching, exposing the bottom oxide barrier layer. Two sets of membranes were fabricated, with different anodization voltages in order to obtain different pore sizes. The resulting mean pore diameter of membranes was of the order of 50 nm, with a separation between pores of 100 nm for the oxalic acid at 50 V, called normal anodization (NA) process and 100 nm of pore sizes with 250 nm of interpore distance by using oxalic acid at 100 V, denominated hard anodization (HA) process.[16] The interpore distance of each sample is directly related to the bumps mean diameter in the oxide barrier layer, which implies that our sample set is composed by hexagonal domes arrangement with 100 and 250 nm of diameter.

A second stage was the deposition of Co/Pd multilayers on the bumpy membranes by sputtering. The multilayers arrangement consists in Pd(1nm)/[Co(0.4nm)/Pd(1nm)]$_{x10}$, covered by an additional 2 nm of Pd to avoid oxidation. The base pressure in the chamber was 8×10^{-7} Torr, and the Ar pressure during deposition was kept at 3 mTorr using 20 sccm Ar flow. Reference samples have been also deposited at the same time on glass substrates, and Hall cross masks of 1 mm width have been used during sputtering for posterior Hall effect measurements in all samples. Hall resistivity measurements have been performed by four-probe method, using Au covered small pogo-pins making electrical contact and using a Keithley source current (6220) and nanovoltmeter (2182A) for temperatures between 4-300K in a closed cryostat system with 5 T of capability (Cryogenic LTD.).

The morphology of the samples was studied with scanning electron microscopy (SEM) Zeiss EVO MA10 and atomic force microscope (AFM) ezAFM from Nanomagnetic Instrument used also as magnetic force microscope (MFM). The hysteresis loops have been measured at room temperature on a homemade Alternating Gradient Force Magnetometer (AGFM).

III. RESULTS AND DISCUSSION

Figure 1.a and 1.b shows the SEM images of the film deposited onto the barrier layer of AAO membranes with 100 nm and 250 nm of interpore distance obtained in the NA and in the HA process respectively. In the SEM image one can observe the film homogeneity and the regular hexagonal arrangement of domes achieved in the double anodization process. The histogram in fig 1.a confirms the dome diameter of ~100 nm for a NA process while the histogram of fig. 1.b. shows ~250 nm dome diameter obtained from the HA process. Fig. 1.c and 1.d shows AFM images with the topology of the samples, and in the inset it is shown the height profile of the nanodomes. It can be observed that in the HA sample the height of the domes is bigger than in the NA sample.

The magnetization curves of the nanodomes and the reference films are shown in Figure 2, where the magnetic field was applied perpendicular to the film plane. The magnetization curve of nanodomes has a larger coercivity than the curve measured in the continuous film. The increase in coercivity can be attributed to different mechanisms of magnetization reversal in the array of nanodomes as compared to the continuous film, where similar results have been observed previously in samples with
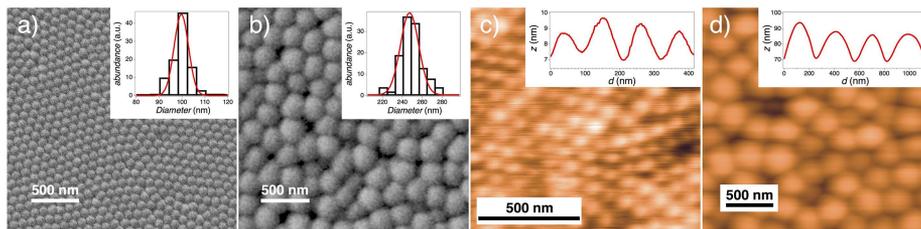

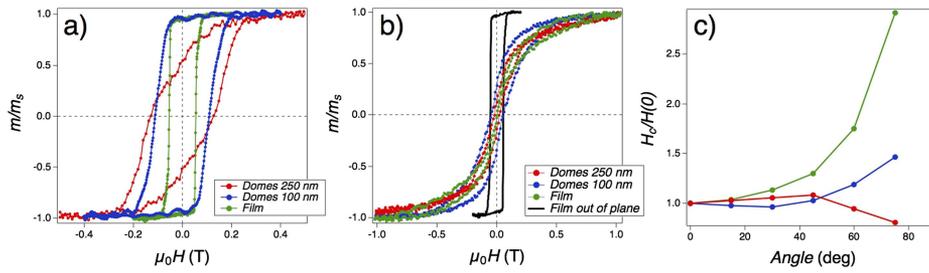FIG. 1. (a), (b) SEM image (c),(d) AFM image of nanodomes film with 100 and 250 nm domes diameter respectively.

FIG. 2. (a) Hysteresis loops of Co/Pd multilayers deposited on glass and nanodomes subtrates with the magnetization parallel to the field, and (b) with magnetization perpendicular to the field. (c) Angular dependence of coercivity for all samples from Hall effect measurements.

out-of-plane anisotropy deposited in nanostructure substrates.[12,13] It is interesting to note that in the HA sample there is a decrease in the magnetic remanence compared with both the film and the sample with nanodomes of 100 nm. This effect could be a direct consequence of the competition of the out of plane with in-plane anisotropies due to the larger curvature of the 250 nm nanodomes, making that the part of the Co/Pd multilayer being deposited in the interstitial space of the domes contribute to decrease the remanence observed. The hysteresis curves measured with field in the plane of the samples are shown in Fig. 2.b., where the out of plane loop of the film is also shown for comparison. From these curves the perpendicular anisotropy of the multilayer film can be estimated as $K_u = 550$ kJ/m^3, where we used the measured values of saturation magnetization $M_s = 700$ kA/m and effective anisotropy field $H_k = 0.7$ T. Angular measurements of coercivity are shown in the Fig. 2.c, where 0 degrees means the magnetic field applied perpendicular to plane direction, i.e., the easy axis of the samples. In the continuous film the coercivity increase just like $1/\cos(\theta)$ as the angle increase, what is attributed to a magnetization reversal by domain wall propagation.[17–19] In the sample with nanodomes of 100 nm the coercivity slightly decrease up to 30 dg and then increases again at higher angles. This behavior has been compared previously to Stoner-Wolfarth reversal mechanism,[20] but as in our case the agreement of the model with the experimental data is not perfect. In the case of sample with nanodomes of 250 nm the coercivity shows almost a constant dependence with angle, what could be a consequence of the larger dispersion of sizes and heights of nanodomes, increasing the anisotropy dispersion over the nanostructure and also the spherical symmetry of the single nanodome.

In order to compare the magnetic domain configuration in both systems, we performed MFM images of the samples in the demagnetized state. The samples were demagnetized using an oscillating applied magnetic field with reduced amplitude. The MFM in the continuous film shows magnetic domains that extends over the whole scanned area of 10 μm x10 μm, as can be seen in figure 3a. These large magnetic domains, forming isotropic labyrinth patterns, were observed previously in Co/Pd multilayers with similar number of bi-layers.[8,21] The MFM images taken in the array of nanodomes with 100 nm shows a completely different pattern, as can be observed in figure 3.b. A pattern of bicolor magnetic domains with opposite magnetization directions is clearly observed, and
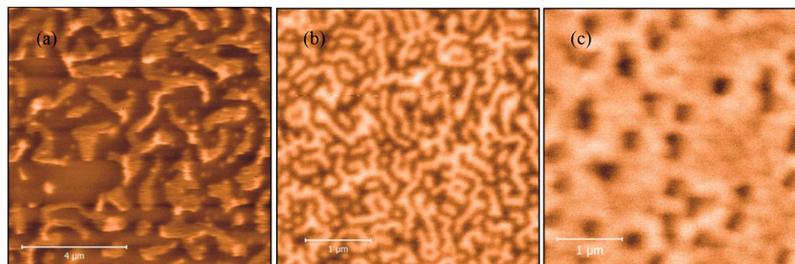

FIG. 3. MFM images of the continuous film (a), the array of nanodomes with 100 nm (b), and the array of 250 nm nanodomes in (c).
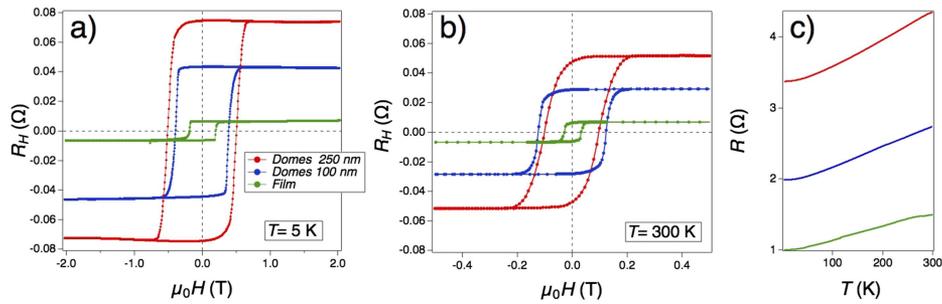
FIG. 4. (a) and (b) Hall resistivity as a function of the applied magnetic field at 5 K and 300 K respectively. (c) Temperature dependence of the resistance of the sample set.

the width of the observed magnetic stripes corresponds exactly to the diameter of the nanodomes. In Figure 3.c it is shown the MFM image for the array of nanodomes with 250 nm in diameter. In this sample the magnetic domains again correspond to the width of the nanodomes, and the magnetic stripes are shorter than the ones observed in Fig. 3.b. The HA sample have a larger dispersion in size and height of nanodomes, and this larger size dispersion can be responsible for the shorter magnetic stripes seen in the MFM image.

Figure 4 shows the Hall resistance versus applied field for the three samples. The following relation gives the Hall resistance R_H in magnetic materials, $R_H = R_0 B + R_s M$, where B is the magnetic induction, M is magnetization and R_0 and R_s are the ordinary and extraordinary Hall coefficients, respectively. The first term is related to the ordinary Hall effect caused by the Lorentz force acting on charge carriers. The second term is related to the magnetization and is called extraordinary Hall Effect (EHE). EHE is usually much larger than the ordinary Hall effect; especially in samples with PMA. Therefore, the Hall resistivity versus field curve resembles the magnetization curve. Actually the concordance of the R_H (H) and M (H) curves is very good for our samples.

In Figure 4 the Hall curves for the nanodomes shows the same increase in coercivity observed in the M(H) curves of Fig. 2, when compared with the continuous film. However, the Hall resistance is almost one order of magnitude larger in the nanodomes with 100 nm, and even larger in nanodomes with 250 nm, as compared to the continuous film. The Hall effect of the samples has been also measured at 5 K, and the corresponding curves are shown in Figure 4.a. The coercivity of the three samples increase at low temperature, as shown in Fig. 4.a, and the coercivity of HA sample becomes larger than the NA sample at 5 K, as opposed to observed at 300 K form. The remanence for HA sample at 5 K is higher compared to the one at 300 K. At low temperature the extraordinary Hall resistance increases only for the samples with nanodomes substrates and the Hall curves have a squarer form. All samples have a metallic behavior as can be observed in the resistance dependence of temperature, shown in Figure 4.c. It is worth to note that the resistance in the films deposited in nanodomes increase as the diameter of the nanodomes increase, at room and low temperatures. One possibility of resistivity increase can be due to an increase of scattering of the electrical current flowing thought the valleys between the nanodomes along the sample. If we focused on fig. 2.a. there exist a difference in the remanence values for the 250 nm diameter nanodomes. This decrease in the magnetization loop can be explained by an anisotropy contribution of the film deposited in the lateral part of the domes. On the other hand, in the Hall effect curve the remanence remains high, indicating that the current is probably not flowing through the lateral part of the domes, remaining in the valleys, where the main contribution to magnetization is normal to the film plane. The dependence of extraordinary Hall resistivity with normal resistivity in Co/Pd multilayers has been studied as a function of number of multilayer repeats.[22] Surface scattering was reported to appear as the thickness of the film decreases bellow 20 repeats, increasing the resistivity and affecting the EHE.[22] Since all samples where deposited at the same time, resulting in the same conditions and thickness, the increase in the resistance, and consequently in the extraordinary Hall resistance in nanodomes could be explained by the increase of scattering due to presence of the domes and possibly to the film discontinuities due to shadowing effects in the valleys of the nanodomes.

IV. CONCLUSION

Co/Pd multilayers have been deposited in continuous films and on the barrier layer of ordered alumina membranes, forming nanodomes with different diameters. The multilayers reproduce the geometry of the nanodomes, and magnetic, structural and electrical properties of the samples have been studied. From MFM images it is possible to observe a decrease in the magnetic domain sizes down to the diameter of the nanodomes, resulting in an increase in the coercivity of the films. In the sample with larger domes the curvature of the substrate decreases the perpendicular anisotropy, as observed by the decrease of the remanence. An increment in the extraordinary Hall effect was observed in the films deposited in nanodomes, as compared to the continuous film. This increase in the Hall resistance can be further exploited, aiming the development of MRAMS and Hall sensors, since a low resistivity can be a limiting factor for development of PMA devices made by metallic films.[4]

ACKNOWLEDGMENTS

[1] P. F. Carcia, A. D. Meinhaldt, and A. Suna, "Perpendicular magnetic anisotropy in Pd/Co thin film layered structures," Applied Physics Letters **47**, 178 (1985).

[2] F. J. A. den Broeder, H. C. Donkersloot, H. J. G. Draaisma, and W. J. M. de Jonge, "Magnetic properties and structure of Pd/Co and Pd/Fe multilayers," J. Appl. Phys. **61**, 4317 (1987).

[3] J.-S. Wi, K. Lim, T. W. Kim, S.-J. Choi, K.-H. Shin, and Ki-B. Kim, "Fabrication of multilayered Co/Pd nano-dot array with an areal density of 1 tera-dot/in^2," J. Magn. Magn. Mater. **322**, 17 (2010).

[4] Moritz, B. Rodmacq, S. Auffret, and B. Dieny, "Extraordinary Hall effect in thin magnetic films and its potential for sensors, memories and magnetic logic applications," Journal of Physics D: Applied Physics **41**, 13 (2008).

[5] J. K. née Moser, V. Kunej, H.-F. Pernau, E. Scheer, and M. Albrecht, "Magnetoresistive effects in Co/Pd multilayers on self-assembled nanoparticles," J. Appl. Phys. **107**, 09C506 (2010).

[6] M. T. Rahman, N. N. Shams, C. H. Lai, J. Fidler, and D. Suess, "Co/Pt perpendicular antidot arrays with engineered feature size and magnetic properties fabricated on anodic aluminum oxide templates," Phys. Rev. B **81**, 014418 (2010).

[7] J. M. Shaw, S. E. Russek, T. Thomson, M. J. Donahue, B. D. Terris, O. Hellwig, E. Dobisz, and M. L. Schneider, "Reversal mechanisms in perpendicularly magnetized nanostructures," Phys. Rev. B **78**, 024414 (2008).

[8] R. Sbiaa, M. Ranjbar and J. Åkerman, "Domain structures and magnetization reversal in Co/Pd and CoFeB/Pd multilayers," J. Appl. Phys. **117**, 17C102 (2015).

[9] D. A. Gilbert, B. B. Maranville, A. L. Balk, B. J. Kirby, P. Fischer, D. T. Pierce, J. Unguris, J. A. Borchers, and K. Liu, "Realization of ground-state artificial skyrmion lattices at room temperature," Nat. Comm. **6**, 8462.

[10] D. Tripathy1 and A. O. Adeyeye, "Perpendicular anisotropy and out-of-plane exchange bias in nanoscale antidot arrays," New Journal of Physics **13** (2011).

[11] W. O. Rosa, M. Jaafar, A. Asenjo1, and M. Vázquez, "Nanostructured Co film on ordered polymer nanohills: A base for novel magnetic nanostructures," Nanotechnology **20**, 7 (2009).

[12] L. Piraux, V. A. Antohe, F. Abreu Araujo, S. K. Srivastava, M. Hehn, D. Lacour, S. Mangin, and T. Hauet, "Periodic arrays of magnetic nanostructures by depositing Co/Pt multilayers on the barrier layer of ordered anodic alumina templates," Appl. Phys. Lett. **101**, 013110 (2012).

[13] T. Hauet, L. Piraux, S. K. Srivastava, V. A. Antohe, D. Lacour, M. Hehn, F. Montaigne, J. Schwenk, M. A. Marioni, H. J. Hug, O. Hovorka, A. Berger, S. Mangin, and F. Abreu Araujo, "Reversal mechanism, switching field distribution, and dipolar frustrations in Co/Pt bit pattern media based on auto-assembled anodic alumina hexagonal nanobump arrays," Phys. Rev. B **89**, 17442 (2014).

[14] H. Masuda and K. Fukuda, "Ordered metal nanohole arrays made by a two-step replication of honeycomb structures of anodic alumina," Science **268**, 5216 (1995).

[15] S. Michea, J. L. Palma, R. Lavín, J. Briones, J. Escrig, J. C. Denardin, and R. L. Rodríguez-Suárez, "Tailoring the magnetic properties of cobalt antidot arrays by varying the pore size and degree of disorder," Journal of Physics D: Applied Physics **47**, 335001 (2014).

[16] Y. Li, Z.Y. Ling, S.S. Chen, and J.C. Wang, "Fabrication of novel porous anodic alumina membranes by two-step hard anodization," Nanotechnology **19**, 22 (2008).

[17] S. Honda, T. Yamakawa, K. Takahashi, and T. Kusuda, "Flux reversal and calculations of hysteresis loops in CoCr sputtered films," Jpn. J. of App. Phys. **27**, 1 (1987).

[18] Y. K. Kim and M. Oliveria, "Magnetic properties of sputtered Fe thin films: Processing and thickness dependence," Journal of Applied Physics **74**, 1233 (1993).

[19] J. S. Gau and C. F. Brucker, "Angular variation of the coercivity in magnetic recording thin films," J. Appl. Phys. **57**, 3988 (1985).

[20] E. C. Stoner and E. P. Wohlfarth, "A mechanism of magnetic hysteresis in heterogeneous alloys," Phil. Trans. R. Soc. Lond. A **240** (1947).

[21] R. Sbiaa, Z. Bilin, M. Ranjbar, H. K. Tan, S. J. Wong, S. N. Piramanayagam, and T. C. Chong, "Effect of magnetostatic energy on domain structure and magnetization reversal in (Co/Pd) multilayers," Journal of Applied Physics **107**, 103901 (2010).

[22] Z. B. Guo, W. B. Mi, R. O. Aboljadayel, B. Zhang, Q. Zhang, P. G. Barba, A. Manchon, and X.X. Zhang, "Effects of surface and interface scattering on anomalous Hall effect in Co/Pd multilayers," Phys Rev B **86**, 104433 (2012).